

# A Topology Simplification Method For 2D Vector Fields

Xavier Tricoche

Gerik Scheuermann

Hans Hagen

University of Kaiserslautern  
Department of Computer Science  
P.O. Box 3049, D-67653 Kaiserslautern  
Germany

E-mail: {tricoche|scheuer|hagen}@informatik.uni-kl.de

## Abstract

Topology analysis of plane, turbulent vector fields results in visual clutter caused by critical points indicating vortices of finer and finer scales. A simplification can be achieved by merging critical points within a prescribed radius into higher order critical points. After building clusters containing the singularities to merge, the method generates a piecewise linear representation of the vector field in each cluster containing only one (higher order) singularity. Any visualization method can be applied to the result after this process. Using different maximal distances for the critical points to be merged results in a hierarchy of simplified vector fields that can be used for analysis on different scales.

**Keywords:** vector field topology, flow visualization, clustering, simplification

## 1 Introduction

Computational Fluid Dynamics (CFD) and fluid mechanics measurements provide scientists and engineers with large vector data sets. A major visualization challenge is to extract essential information for interpretation. Vector field topology [6, 4] creates a graph consisting of all critical points and separatrices resulting in a dense structure description. The background is given by the qualitative theory of differential equations due to Poincaré [9]. This method has been very successful since it automates the visualization process of large vector data sets and dramatically reduces the presented information.

For turbulent flows, however, topology-based methods lead to cluttered pictures usually preventing the user from large scale qualitative analysis. Since turbulent flows are characterized by a large number of close vortices of different scales, we like to develop a description with a reduced number of critical points that still contains the topological information of the given data set. This leads to methods for vector field topology simplification. Our central idea is to merge close critical points into one, potentially higher order, critical point. This reduces the clutter, but it keeps the topology consistent.

The described method starts with a planar piecewise bilinear structured grid. We locate all critical points in an usual zero search over the cells. Then, we partition the grid into convex cell clusters, called *supercells*. In each supercell, the distances between the critical points must be below a prescribed value. We use a typical top-down clustering approach starting with the whole grid as first cluster and successive subdivision until all clusters obey the rule. Now, we know which critical points to merge. Since we want to have a piecewise analytic description of our vector field, we have to modify the internal supercell geometry and/or interpolation. We choose the grid point closest to the center of all critical points in the supercell and set its vector value to zero. Then, we connect all grid points from the supercell boundary to this point. This results

in a new mesh that has exactly one critical point in each supercell. Since this critical point is on a vertex in a piecewise linear field, we may produce a higher order critical point of arbitrary complexity. Essentially, we concentrate the preexisting topological flow properties in a single point. In this sense, our grid modification acts as a fusion of all singularities in the supercell.

The analysis of the resulting higher order singularity requires a generalization of the usual critical point analysis, since there is no valid derivative at a grid vertex. The general idea goes back to work by Andronov et al. [1]. It is based on a partition of the neighborhood of the critical point into sectors of different behavior. The sequence of these sectors defines the topological type of the critical point. The sectors are divided into three types: hyperbolic, parabolic and elliptic. A hyperbolic sector contains only streamlines that pass the critical point without approaching it. The simple case is a saddle point with its four hyperbolic sectors. A parabolic sector consists of streamlines that start/end at the critical point and end somewhere else. Simple sources or sinks have only parabolic sectors. Finally, elliptic sectors consist of streamlines that loop back to the critical point, i. e. that start and end at this point. There are no elliptic sectors in a linear vector field, but one may imagine a simple dipole with two elliptic sectors. We present the details on definitions and analysis including calculating the separatrices in later sections.

We use a simple analytic case to verify the analysis and explain the results of the basic algorithm. Our application is a axisymmetric turbulent jet simulation with more than 300 critical points. We show the simplification for two different values of the radius to give an impression of the simplification in the topology graph.

## 2 Related Work

A multiresolution approach of 2D vector fields over curvilinear grids was introduced in [8] to simplify the flow by eliminating the visual clutter caused by higher order details. Yet, this method does not focus on the topology and is not designed to ensure a prescribed accuracy in the topological graph approximation.

W. de Leeuw et al. [3] addressed the issue of vector field topology simplification last year. Their method simplifies the topological graph by successive removal of connected pairs of critical points. The authors achieve a significant reduction of the number of critical points, simplifying the corresponding topological structure. The method does not give a description of the simplified vector field. Therefore, it cannot be combined with methods like LIC [2] to show the results of the simplification. Furthermore, it is unable to simplify arbitrary topological configurations, since it does not create higher order critical points.

The problem of detecting higher order critical points was discussed by G. Scheuermann et al. [11]. This paper suggests the use of polynomial approximations to allow higher order singularities inside cells. The detection is based on a search for several close

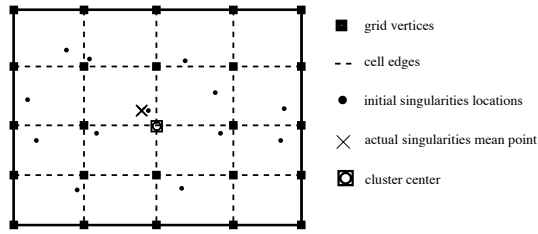


Figure 1: Cluster singularities and cluster center

simple critical points in a piecewise linear interpolation, since this might indicate the existence of more complicated features in the underlying real field.

A cluster based simplification of vector fields has been presented by B. Heckel et al. [5]. It avoids the use of cell connectivity during the simplification process and is able to reduce the size of large 3D vector data sets substantially. The field simplification is monitored by the deviation of streamlines starting at the original discrete vector positions from their counterparts in the original vector field. However, no attention is paid to the change of vector field topology, so qualitative consistency may be lost.

### 3 Cells Clustering

This section discusses grouping cells to get a domain decomposition into cell groups that contain only close singularities. This is a typical clustering problem with the proximity of contained singularities as criterion. To solve it, we have adapted an algorithm proposed by T. Schreiber [10] originally designed for computational geometry. In particular, we had to adapt the method so that it can handle grid cells. Let us first introduce some convenient notations. (For simplicity, we deal in this section with a structured grid mapped in a computational space to a rectilinear grid). We denote by  $P_1, \dots, P_m$  the positions of the  $m$  singularities lying inside a particular cluster. We want to minimize the approximation error of these  $m$  singularities by a single point, where this point (or cluster center)  $Q$  is chosen to be the best approximation (for a given norm) of the singularities (see Fig. 1). The corresponding error is

$$S = \frac{\sum_{j=1}^m \omega_j \|P_j - Q\|}{\sum_{j=1}^m \omega_j}$$

where  $\omega_i$  is the weight (set equal to 1 in our case) associated with the  $i$ th singularity. So the aim of the clustering process is to get a set of clusters that all have an error value smaller than a specified threshold (which is the only parameter of our method) and that cover the whole grid.

If a cluster does not satisfy the given error criterion, we split it into subclusters. To do this, we need to introduce the projected variances associated with a given cluster:

$$V_i = \sum_{j=1}^m \omega_j (P_j^i - Q^i)$$

where  $i \in 0, 1$  is the considered coordinate axis ( $P_j = (P_j^0, P_j^1)$ ).

Now, considering the whole grid as initial cluster, the method is as follows.

**Step 1.** Take as cluster center the best vertex approximation of all cluster singular points.

**Step 2.** Compute the approximation error  $S$ .

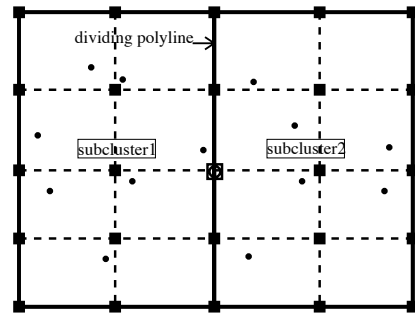


Figure 2: Cluster splitting

If ( $S > \text{THRESHOLD}$ ) go to step 3.  
Otherwise stop.

**Step 3.** Compute the coordinate axis with largest projected variance (i.e.  $\max(V_0, V_1)$ ).

**Step 4.** Create 2 subclusters by splitting the cluster at an edge polyline through  $Q$  perpendicular<sup>1</sup> to the selected coordinate axis.  
For each cluster, go to step 1.

Step 4 justifies the need for a cluster center to be a grid vertex. As a matter of fact, when splitting a cluster, we keep processing cell groups in the form of Fig. 2. To ensure that the algorithm terminates, we used the existence of a best singularity mean point approximation by a grid vertex that does not lie on the cluster boundary as additional criterion.

## 4 Topology Simplification

### 4.1 Local Cell Structure Modification

Once the close singularity clusters have been determined, we have to remodel the topology inside each supercell to simplify the resulting topology graph. As mentioned previously, we aim at simulating the fusion of all cluster singularities at their mean point. This fusion process may be thought of as bringing all singular points arbitrary close together. Nevertheless, this action should remain local because topological consistency must be preserved. Consequently, we leave the field unchanged along the cluster boundary. Indeed, to be consistent, we have to ensure that the index computed along a curve enclosing all cluster singularities remains unchanged after deformation (see [1], chapt. V, for a presentation of the Poincaré index theory). This is guaranteed if the cluster boundary itself remains unchanged. So the desired topology deformation is a new analytic field description inside the cluster that fits the original field value on the boundary edges and that contains no other singularity than the one artificially created in order to synthesize the topological “action” of the preexisting singularities. We have already mentioned that the kind of data we process lies on a structured bilinear interpolated grid, thus the field value on the boundary has to be piecewise linear. So inside the cluster, we remove all the preexisting quadrilateral cells and cover the resulting empty domain with triangles joining the mean point to the cluster boundary as shown in Fig. 3.

The new singularity should be located at the center vertex (mean point), so we give this vertex the vector value zero. Every new triangle is linearly interpolated. Now a well-known property of a

<sup>1</sup>in computational space

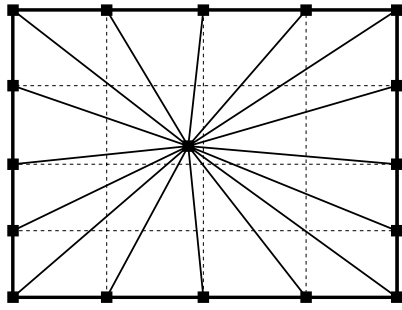


Figure 3: New cell structure in the cluster

linear vector field is that it contains at most one singular point. So in each triangle, the “intern” vertex is the only location of a singular point. At last, the edges on the cluster boundary keep the linear interpolation so the vector values are unchanged. Consequently, the new intern structure fulfills all requirements.

## 4.2 Local Topology Analysis

### 4.2.1 Sector Types

At this stage, we need a definition of a topology graph that is general enough to handle the case of zero vectors lying at a intern vertex of a piecewise linear interpolated supercell.

As a matter of fact, the classical definition of the topological graph, as given in [6], supposes that all singular points of the vector field are of linear type (we say of first order) (see [7], pp. 92-96, for a classification of the linear singularities). If this is the case, the topology graph (or *skeleton*) is defined as the graph built up of all singular points and the integral curves (or streamlines) starting or ending at saddle points along the eigenvectors and integrated until they reach the domain boundary, another singular point or a cycle orbit. Note that we do not deal with cycle orbits in this paper (see [12]). This definition is actually a special case of the general definition as we will see.

In the following, we use the theoretical results of [1]. In the classification of possible singularity types, the authors distinguish singular points that are reached by no integral curve (called *center type*) from those that are reached by at least one streamline (*non center type*).

**Center Type** In this case, one can find a neighborhood of the singular point where all integral curves are closed, inside one another, and contain the singular point in their interior as shown in Fig. 4.

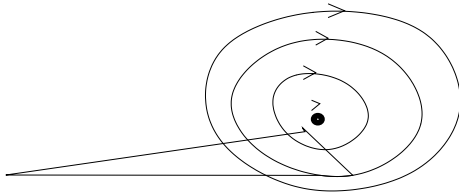


Figure 4: Center type

**Non Center Type** In this case, one does not only have a single integral curve converging to the singular point but actually two at least. To analyze the local structure of such a singularity, we have to

consider the behavior of all streamlines passing through its neighborhood. This neighborhood is made of several **curvilinear sectors** (see Fig. 5).

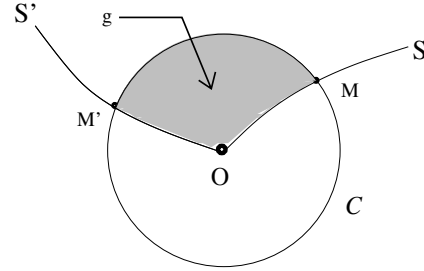


Figure 5: Curvilinear sector

A curvilinear sector is defined as the region bounded by a circle  $C$  with arbitrary small radius and two streamlines  $S$  and  $S'$  both converging (for either  $t \rightarrow \infty$  or  $t \rightarrow -\infty$ ) towards  $O$ . One then considers the streamlines passing through the open sector  $g$  in order to distinguish between three possible types of curvilinear sectors.

- Case 1.  $S$  tends to  $O$  for  $t \rightarrow \infty$  and  $S'$  tends to  $O$  for  $t \rightarrow -\infty$ : Every integral curve passing through the open sector  $g$  leaves  $g$  for both  $t \rightarrow \infty$  and  $t \rightarrow -\infty$ . The sector is called a **hyperbolic** or **saddle sector**.

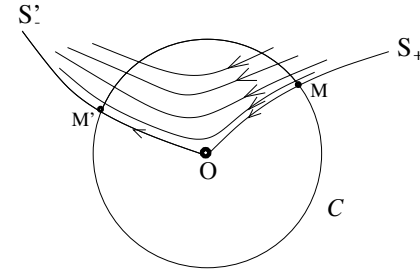


Figure 6: Hyperbolic sector

- Case 2.  $S$  and  $S'$  both tend to  $O$  for  $t \rightarrow \infty$  (resp.  $t \rightarrow -\infty$ ): Every integral curve through the open sector  $g$  tends to  $O$  for  $t \rightarrow \infty$  (resp.  $t \rightarrow -\infty$ ) without leaving  $g$  and leaves  $g$  for  $t \rightarrow -\infty$  (resp.  $t \rightarrow \infty$ ). The sector is known as a **parabolic sector**.

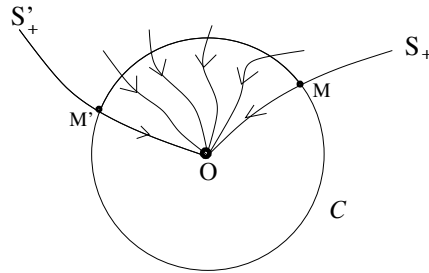


Figure 7: Parabolic sector

- Case 3.  $S$  and  $S'$  are two semi-integral curves on the same integral curve: All the paths through a point inside this loop form nested loops tending to  $O$  for both  $t \rightarrow \infty$  and  $t \rightarrow -\infty$ . The sector is called an **elliptic sector**.

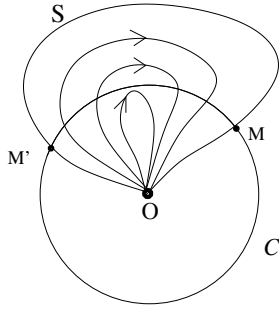


Figure 8: Elliptic sector

Now, in the general case, **separatrices** are defined as streamlines that are boundary curves of a hyperbolic sector. To determine the local topology of a singularity, we have to get the type of its different curvilinear sectors and retain the boundary curves of the hyperbolic ones. Obviously, if all singular points are of first order, the only singularities presenting hyperbolic sectors are saddle points and we are thus consistent with the former definition.

#### 4.2.2 Finding Separatrices

In order to locate the position of our separatrices, we use the following (straightforward) property (see Fig. 9).

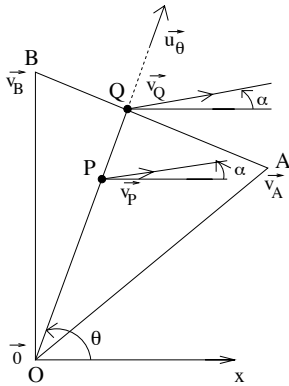


Figure 9: Linear vector field in polar coordinates

**Property 4.1** Taking the singularity as origin, the orientation of the vector field does not depend on the radius. That is, one has:

$$\vec{v}(r, \theta) = f(r, \theta) \cdot \vec{v}(\theta)$$

where  $f(r, \theta) > 0$ .

This property has two fundamental corollaries:

**Corollary 4.1** The whole required information for the singularity analysis can be read directly on the supercell boundary.

**Corollary 4.2** Separatrices are in our case streamlines that tend to the singular point along straight lines from the supercell boundary.

Consequently, we are seeking points where the vector field is either parallel or orthogonal to the coordinate vector along the cluster boundary (the further analysis of the “orthogonal” points is required

for the sector type determination, as shown below). Practically, for each linear interpolated edge  $[AB]$  on the cluster boundary one has

$$\begin{cases} \vec{v}(A) = \vec{v}_A \\ \vec{v}(B) = \vec{v}_B \\ \vec{v}(A + t(B - A)) = \vec{v}_A + t(\vec{v}_B - \vec{v}_A), \text{ where } 0 \leq t \leq 1 \end{cases}$$

Thus, if the singularity is taken as coordinates origin, the vector field is parallel to the coordinate vector at  $P := A + t(B - A)$  if and only if

$$\vec{OP} \wedge \vec{v}(P) = 0 \quad (\text{cross product is zero})$$

which is a quadratic equation in  $t$ .

The solutions P are then classified as follows.

- If  $\langle \vec{OP}, \vec{v}(P) \rangle > 0$ , then P is marked PARALLEL+
- Otherwise, P is marked PARALLEL-

Likewise, the vector field is orthogonal to the coordinate vector at P if and only if

$$\langle \vec{OP}, \vec{v}(P) \rangle = 0 \quad (\text{scalar product is zero})$$

which is as well a quadratic equation in  $t$ .

The solutions P are then classified as follows.

- If  $\vec{OP} \wedge \vec{v}(P) > 0$ , then P is marked ORTHOGONAL+
- Otherwise, P is marked ORTHOGONAL-

That is, in both cases, we have to solve a quadratic scalar equation. The (possible) real roots must next be checked between 0 and 1 to describe a point actually lying on the considered edge. Once the found points have been sorted, we use the graph in Fig. 10 to determine the nature of the different sectors and locate the boundary curves of the hyperbolic ones. Note that a boundary curve between an elliptic and a parabolic sector cannot be determined locally but proceeds from the global field topology as a separatrix emanating from another singular point. An illustration of the definitions above

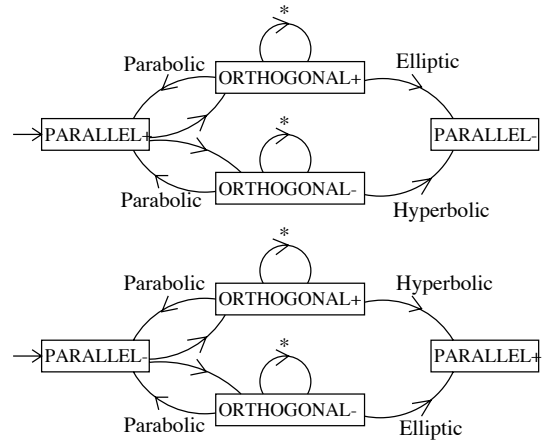


Figure 10: Sectors discrimination graph

is proposed in Fig. 11.

## 5 Results

In this section, we apply our topology simplification method to a 2D polynomial vector field as well as to a simulation of a swirling jet.

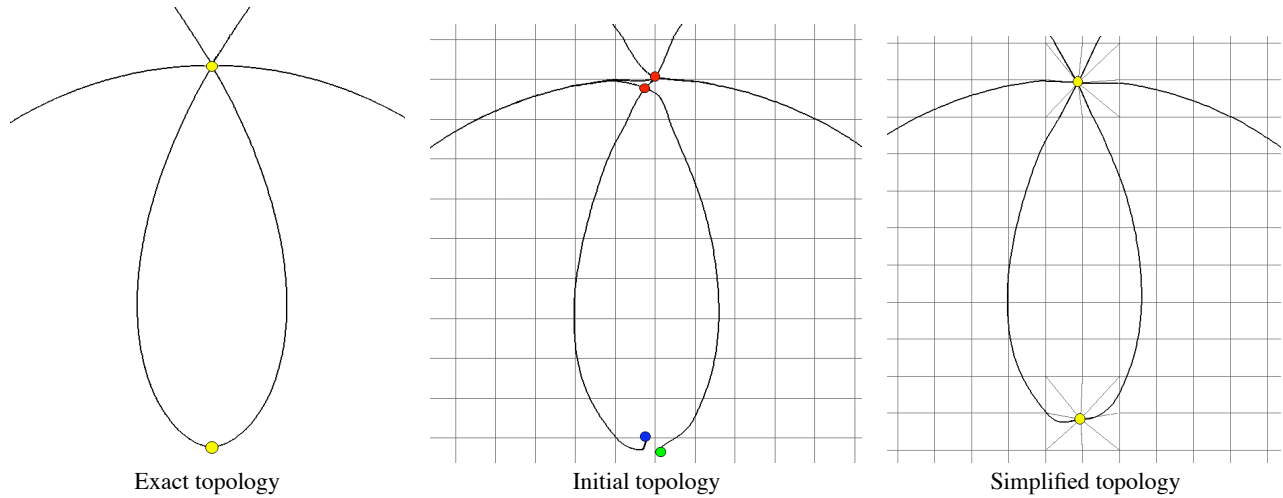


Figure 12: Application to an analytic vector field

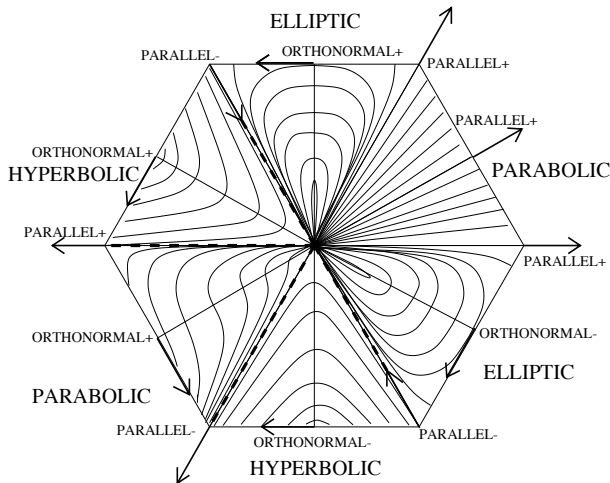


Figure 11: Example of sector type identification

## 5.1 Analytic Vector Field

This polynomial example has been designed with Clifford algebra. It consists of two topological features (a monkey saddle and a dipole) that are joined by the separatrices as shown in Fig. 12, on the left. The interest of these two features is that they are of higher order and thus cannot be handled properly by classical topology extraction methods with linear precision. Furthermore, they cannot occur in a piecewise bilinear interpolated vector field. Sampling this field on a  $20 \times 20$  structured grid, we observe this deficiency: We obtain a topology where 4 critical points are present (the monkey saddle has been split into two saddle points and the dipole into a sink and a source, see in the middle). Processed with a threshold of 0.3, the simplification is as shown on the right: The source and sink have been merged in a dipole while both saddles have been merged in a monkey saddle. The local topology analysis of the dipole reveals 2 elliptic and 2 parabolic sectors whereas the monkey saddle presents 6 hyperbolic sectors and therefore is reached by 6 separatrices that form the depicted topological graph. That is, the original features have been recovered. The grid has been displayed to show

how the clustering works.

More generally, this example shows that, when higher order singular points are in the real vector field, our method can be used to attack the “splitting effect” of low-order interpolants and to restore the original nature of the topological features because of its ability to handle critical points of any type.

## 5.2 Swirling Jet

This example is a simulation of a swirling jet with an inflow into a steady medium. It results in a vortex breakdown. Here one wants to investigate the turbulence of the vector field. The grid is structured and has  $251 \times 159$  cells ranging from 0 to 15 in  $x$ , resp.  $-1.9$  to  $1.9$  in  $y$ . The initial topology has a very complicated structure and contains 337 singular points. The many singularities lead into visual clutter so that the topological information cannot be efficiently interpreted. Figure 13 shows the initial topology together with the results of our method applied with two different thresholds. Furthermore, three enlargements are proposed that give an insight into the local effect of the method. With 0.2 taken as threshold, we get 140 critical points (88 merged ones) and with 0.4, the topology contains 88 critical points (in this case, only 6 are simple singularities!). It follows that the corresponding pictures appear clarified and the streamline paths easier to track while for both thresholds the global structure has been respected. Furthermore, a very interesting property is the preserved symmetry in the simplified fields. This is due to the clustering method and the split strategy depending on the maximal projected variance (see section 3).

At last, to demonstrate the effect of our method on the flow itself, we give in Fig. 14 the LIC pictures corresponding to the simplified topologies proposed in Fig. 13.

## 6 Conclusions

We have presented a method that simplifies the topology of a vector field defined on a 2D structured grid while providing a piecewise analytic description for the simplified field. It is based upon the fusion of close simple singularities into a higher order critical point presenting a similar structure in the large. The groups of singularities that will be merged is first supplied by a clustering strategy that works on the grid cells. The merging process is next the result of

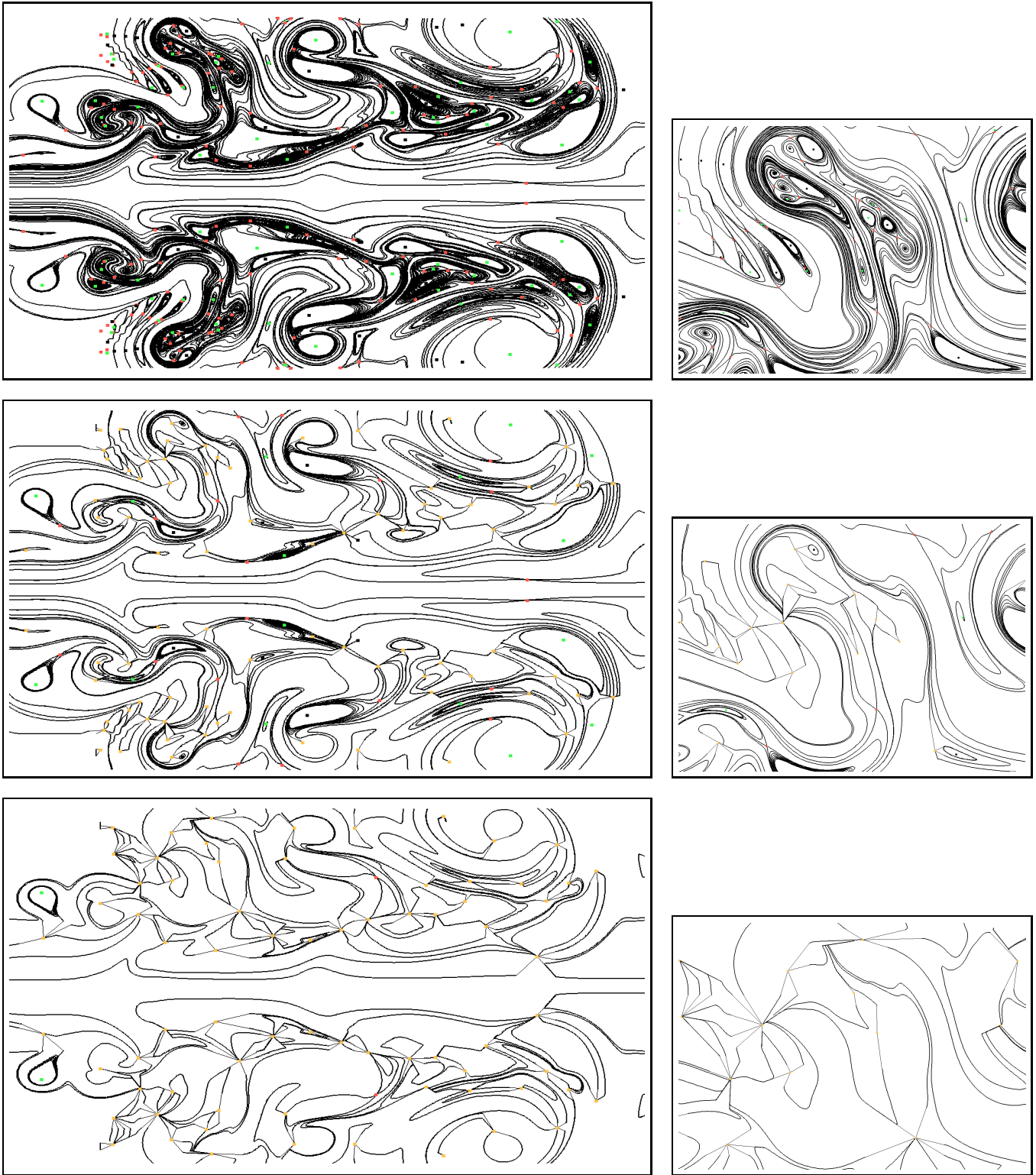


Figure 13: Topology scaling: initial graph and simplifications with 0.2 and 0.4 as threshold

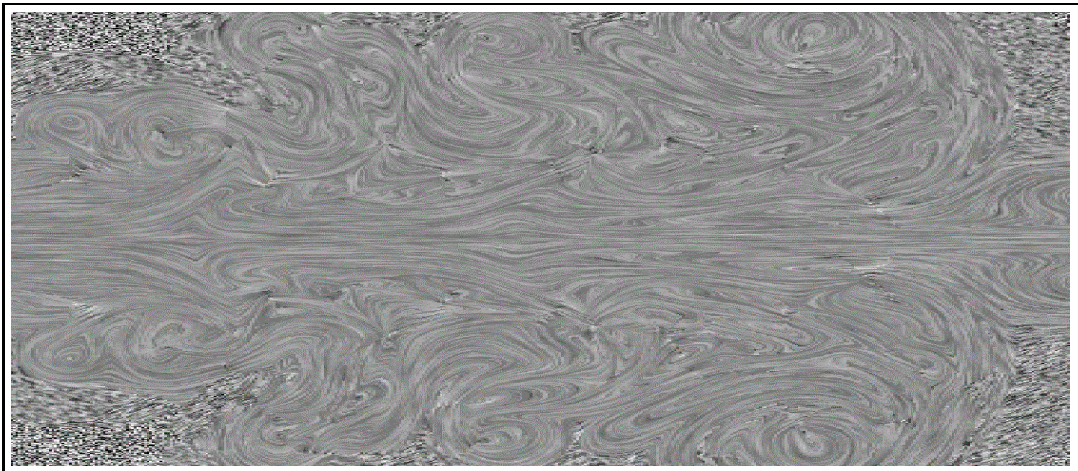
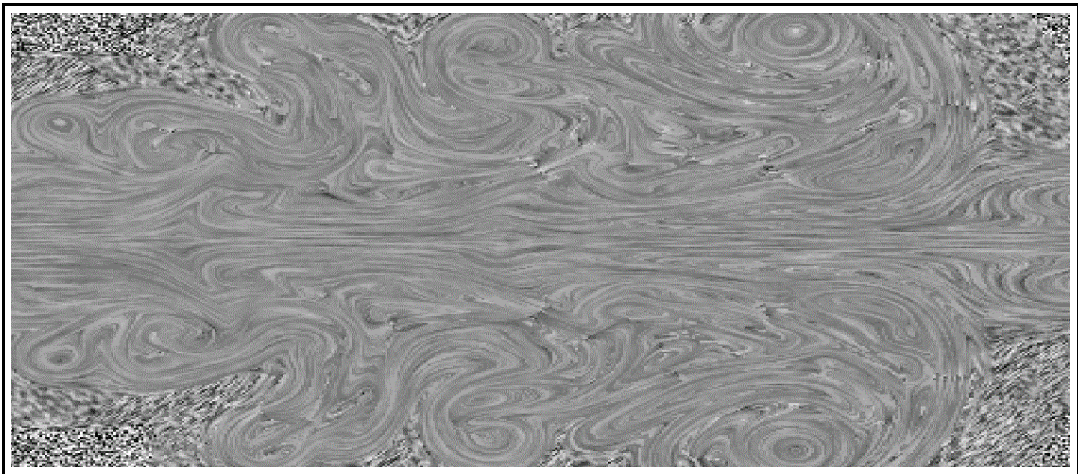
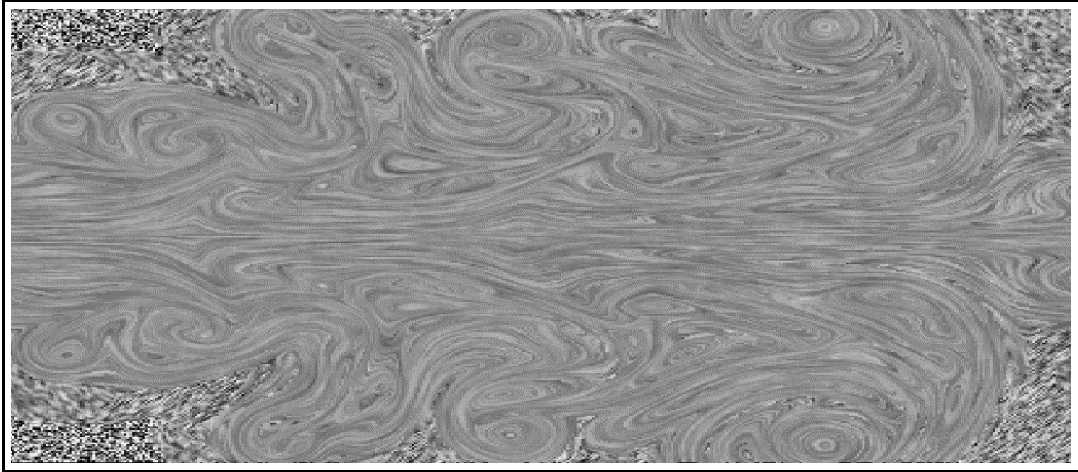


Figure 14: Topology scaling: initial LIC picture and simplifications with 0.2 and 0.4 as threshold

a local grid deformation inside each cluster that preserves the field continuity. We achieve thus a significant reduction of the number of singular points which clarifies the topological graph while keeping the initial topological information, as demonstrated by our example. By considering an analytic vector field, we have also shown that our method can be used to restore in an interpolated vector field higher order singular points suspected in the real flow.

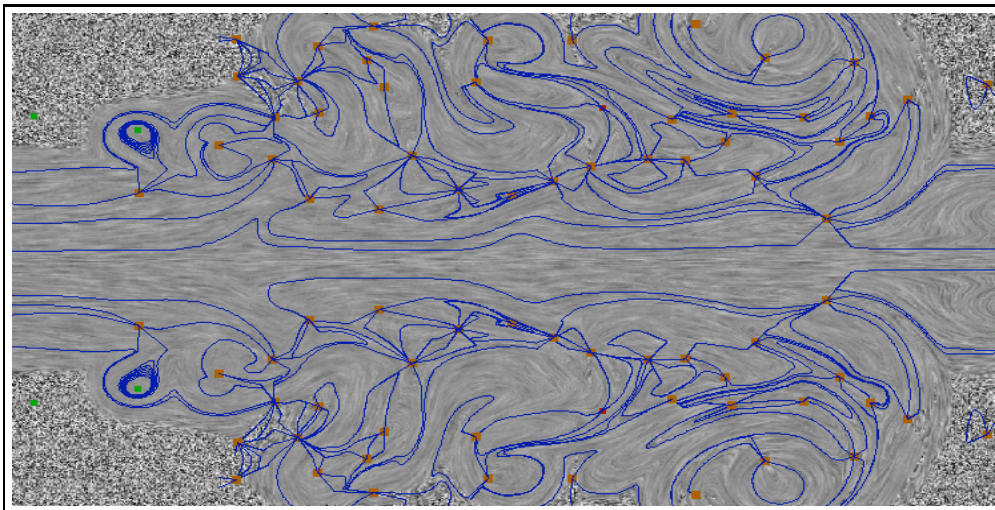
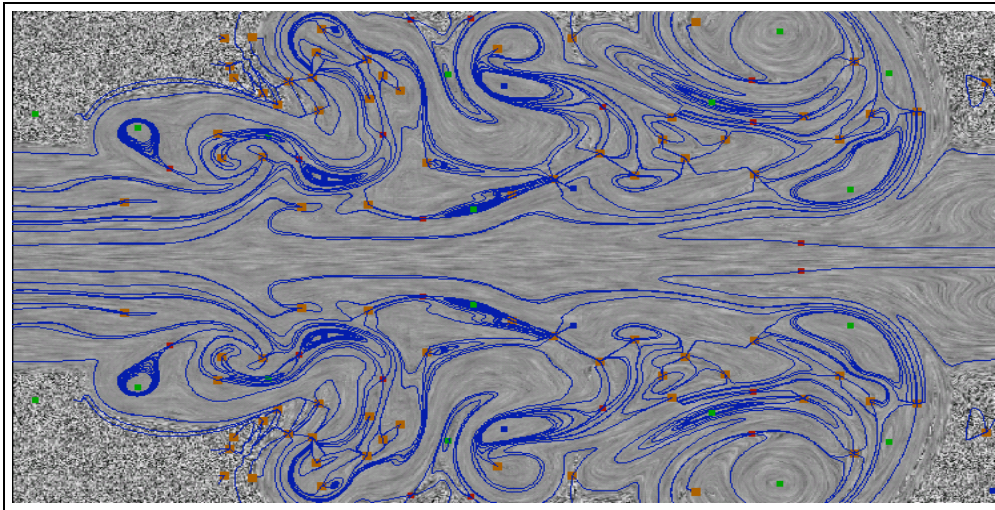
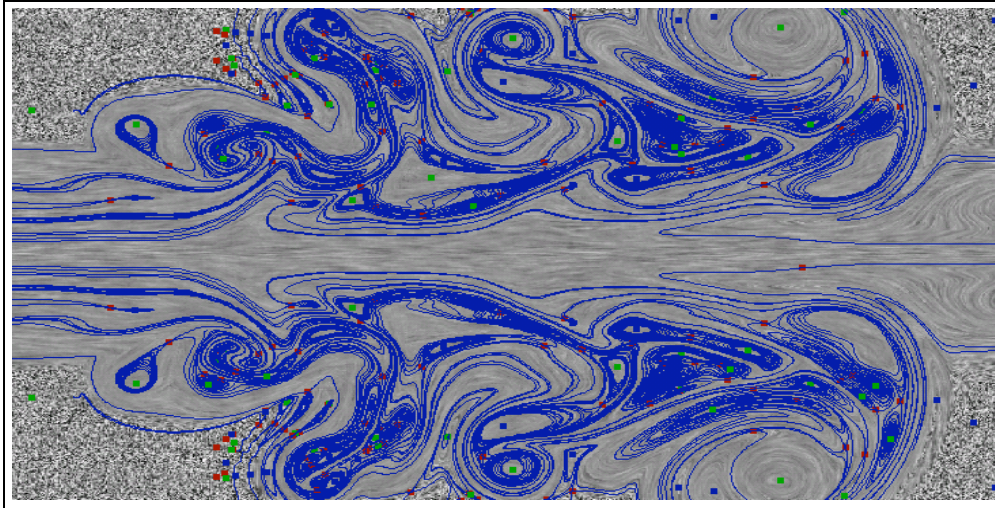
## Acknowledgments

This research was supported by the DFG project “Visualisierung nicht-linearer Vektorfeldtopologie”. The Authors wish to thank Wolfgang Kollmann, MAE Department of the University of California at Davis, for providing the swirling jet dataset. Furthermore, we would like to thank Tom Bobach, Holger Burbach, Jan Frey, Aragorn Rockstroh, René Schätzl and Thomas Wischgoll for their programming effort.

## References

- [1] Andronov A.A., Leontovich E.A., Gordon I.I., Maier A.G., *Qualitative Theory of Second-Order Dynamic Systems*. Israel Program For Scientific Translation, Halsted Press, 1973.
- [2] Cabral B, Leedom L., *Imaging Vector Fields Using Line Integral Convolution*. In SIGGRAPH '93 Proceedings, ACM, New York, NY, 1993, pp. 263-270.
- [3] de Leeuw W., van Liere R., *Collapsing Flow Topology Using Area Metrics*. In Proceedings of IEEE Visualization '99, IEEE Computer Society, San Francisco, CA, 1999, pp. 349-354.
- [4] Globus A., Levit C., Lasinski, T., *A Tool for Visualizing of Three-Dimensional Vector Fields*. In Proceedings of IEEE Visualization '91, IEEE Computer Society, San Diego, CA, 1991, pp. 33-40.
- [5] Heckel B., Weber G., Hamann B., Joy K.I., *Construction of Vector Field Hierarchies*. In Proceedings of IEEE Visualization '99, IEEE Computer Society, San Francisco, CA, 1999, pp. 19-25.
- [6] Helman J.L., Hesselink L., *Visualizing Vector Field Topology in Fluid Flows*. IEEE Computer Graphics and Applications, 1991.
- [7] Hirsch M.W., Smale S., *Differential Equations, Dynamical Systems and Linear Algebra*. Academic Press, 1974, pp. 89-96.
- [8] Nielson G.M., Jung I.H., Song, J., *Wavelets over Curvilinear Grids*. In Proceedings of IEEE Visualization '98, IEEE Computer Society, Research Triangle Parck, NC, 1998, pp. 313-317.
- [9] Poincaré H., *Sur les courbes définies par une équation différentielle* Oeuvres, Vol. I., Paris, Gauthier-Villars, 1928.
- [10] Schreiber T. *A Voronoi Diagram Based Adaptive K-Means-Type Clustering Algorithm for Multidimensional Weighted Data*. Lecture Notes in Computer Science 553, H. Bieri, H. Noltemeier (Eds.), Computational Geometry - Methods, Algorithms and Applications. Springer Verlag 1991, pp. 265-275
- [11] Scheuermann G., Hagen H., Krüger H., Menzel M., Rockwood A.. *Visualization of Higher Order Singularities in Vector Fields*. In Proceedings of IEEE Visualization '97, IEEE Computer Society, Los Alamitos, CA, 1997, pp. 67-74.
- [12] Wischgoll T., Scheuermann G., *Detection and Visualization of Closed Streamlines in Planar Fields*. Submitted for publication





Topology scaling: LIC picture and topology for 0, 0.2 and 0.4 as simplification thresholds